Journal of Visualized Experiments
Magnetic adjustment of afterload in engineered heart tissues
--Manuscript Draft--

Article Type:	Invited Methods Article - JoVE Produced Video
Manuscript Number:	JoVE60811R1
Full Title:	Magnetic adjustment of afterload in engineered heart tissues
Section/Category:	JoVE Bioengineering
Keywords:	Tissue engineering; engineered heart tissue; cardiac hypertrophy; magnetics; afterload; contraction
Corresponding Author:	Marc Hirt, MD, PhD Universitatsklinikum Hamburg-Eppendorf Hamburg, HH GERMANY
Corresponding Author's Institution:	Universitatsklinikum Hamburg-Eppendorf
Corresponding Author E-Mail:	m.hirt@uke.de
Order of Authors:	Becker Benjamin
	Marita Lynn Rodriguez
	Tessa Ruth Werner
	Justus Stenzig
	Thomas Eschenhagen
	Marc Nikolaus Hirt, MD, PhD
Additional Information:	
Question	Response
Please indicate whether this article will be Standard Access or Open Access.	Standard Access (US$2,400)
Please indicate the **city, state/province, and country** where this article will be **filmed**. Please do not use abbreviations.	Hamburg, Germany

1   **TITLE:**
2   **Magnetic Adjustment of Afterload in Engineered Heart Tissues**
3

4   **AUTHORS AND AFFILIATIONS:**
5   Benjamin Becker[1,2]*, Marita L. Rodriguez[1,2]*, Tessa R. Werner[1,2], Justus Stenzig[1,2], Thomas
6   Eschenhagen[1,2], Marc N. Hirt[1,2]
7

8   [1]Institute of Experimental Pharmacology and Toxicology, University Medical Center Hamburg-
9   Eppendorf, Hamburg, Germany
10   [2]DZHK (German Centre for Cardiovascular Research), partner site Hamburg/Kiel/Lübeck,
11   Germany
12   *Equal author contribution to this work.
13

14   **Email addresses of co-authors:**
15   Benjamin Becker (6693850@stud.uke.uni-hamburg.de)
16   Marita L. Rodriguez (m.rodriguez@uke.de)
17   Tessa R. Werner (tewerner@uke.de)
18   Justus Stenzig (j.stenzig@uke.de)
19   Thomas Eschenhagen (t.eschenhagen@uke.de)
20

21   **Corresponding author:**
22   Marc N. Hirt (m.hirt@uke.de)
23

24   **KEYWORDS:**
25   Tissue-engineering, engineered heart tissue, cardiac hypertrophy, magnetics, afterload,
26   contraction.
27

28   **SUMMARY:**
29   This protocol provides detailed methods describing the fabrication and implementation of a
30   magnetics-based afterload tuning platform for engineered heart tissues.
31

32   **ABSTRACT:**
33   Afterload is known to drive the development of both physiological and pathological cardiac
34   states. As such, studying the outcomes of altered afterload states could yield important insights
35   into the mechanisms controlling these critical processes. However, an experimental technique
36   for precisely fine-tuning afterload in heart tissue over time is currently lacking. Here, a newly
37   developed magnetics-based technique for achieving this control in engineered heart tissues
38   (EHTs) is described. In order to produce magnetically responsive EHTs (MR-EHTs), the tissues are
39   mounted on hollow silicone posts, some of which contain small permanent magnets. A second
40   set of permanent magnets is press-fit into an acrylic plate such that they are oriented with the
41   same polarity and are axially-aligned with the post magnets. To adjust afterload, this plate of
42   magnets is translated toward (higher afterload) or away (lower afterload) from the post magnets
43   using a piezoelectric stage fitted with an encoder. The motion control software used to adjust
44   stage positioning allows for the development of user-defined afterload regimens while the

45 encoder ensures that the stage corrects for any inconsistencies in its location. This work describes
46 the fabrication, calibration, and implementation of this system to enable the development of
47 similar platforms in other labs around the world. Representative results from two separate
48 experiments are included to exemplify the range of different studies that can be performed using
49 this system.
50
51 **INTRODUCTION:**
52 Afterload is the systolic load on the ventricle after it has begun to eject blood[1]. During cardiac
53 development, an appropriate afterload is of critical importance for cardiomyocyte maturation[2].
54 In adulthood, low levels of ventricular afterload (e.g., in bedridden patients with high-level spinal
55 cord injury[3] or in very special cases like spaceflight[4]) can result in hypotrophy of the heart.
56 Conversely, high afterload can lead to cardiac hypertrophy[5]. While cardiac hypertrophy in
57 endurance athletes or pregnant women is considered beneficial and physiological, hypertrophy
58 associated with long-term arterial hypertension or severe aortic valve stenosis is detrimental as
59 it predisposes one to cardiac arrhythmias and heart failure[6]. Although the 5-year mortality rate
60 for heart failure patients has reduced from ~70% in the 1980s[6] to 40–50%[7] presently, there is still
61 a great need for new therapeutic treatment options for this highly prevalent condition (currently
62 2.2% of the population in the Western world)[8].
63
64 In order to investigate the molecular mechanisms of pathological cardiac hypertrophy and to test
65 preventive or therapeutic strategies for treating this disease, in vivo models of afterload have
66 been developed[9-12]. While these models have offered beneficial insights into the effects of
67 afterload on ventricular performance, they do not allow for fine control over afterload
68 magnitude. Alternatively, in vitro studies of afterload performed on excised hearts and muscle
69 preparations allow for finer control over tissue loading, but these models are not conducive to
70 longitudinal studies[13-15].
71
72 To overcome these issues, we developed an in vitro model of elevated afterload in engineered
73 heart tissues (EHTs)[16,17]. This model is a 3-dimensional culture format for rat heart cells
74 embedded in a fibrin matrix suspended between flexible hollow silicone posts. These tissues beat
75 spontaneously (against the resistance of the silicone posts) and perform auxotonic work. We
76 have increased afterload applied to EHTs by a factor of 12 in previous experiments by the
77 insertion of rigid metal braces into the hollow silicone posts for one week. This led to a multitude
78 of changes, characteristic of pathological cardiac hypertrophy[18-20]: cardiomyocyte hypertrophy,
79 partial necroptosis, a decline in contractile force, the impairment of tissue relaxation,
80 reactivation of the fetal gene program, a metabolic shift from fatty acid oxidation to anaerobic
81 glycolysis, and an increase in fibrosis. Though this procedure has been successfully employed in
82 several studies[17,21,22], it has some disadvantages. There are only two states, low or very high (12-
83 fold) afterload, and the procedure requires manual handling of the EHTs, which limits its
84 temporal flexibility and poses the risk of contamination.
85
86 Recently, Leonard et al. used a similar technique to modulate afterload in EHTs cultured on
87 silicone posts[23]. Braces of varying lengths were placed around the outside of the posts to restrict
88 their bending motion. The authors of this study reported that a singular small-to-medium

89 increase in load enhanced force development and maturation of human iPS-derived EHTs, while
90 higher loads resulted in a pathological state. However, similar to our own system, this technique
91 only allows for singular increases in afterload, the magnitude of which is dictated by the length
92 of the braces. As such, fine alterations in afterload, modifications in afterload over time, and
93 precise loading regimens are not possible with these techniques.
94
95 Here, we provide the protocol for a system that can be used to modulate post-resistance, i.e.,
96 afterload of EHTs magnetically[24]. This platform facilitates the fine-tuning of afterload, enables
97 user-defined afterload regimens, and ensures EHT sterility.
98
99 **PROTOCOL:**
100
101 **1. Preparation of the afterload tuning platform**
102
103 NOTE: The steps involved in this portion of the protocol are not time-sensitive.
104
105 1.1. Manufacturing the magnetically responsive silicone racks
106
107 NOTE: These racks serve as the culture platform for EHTs. Each EHT is suspended between two
108 silicone posts, which impart afterload to the tissue. The degree of afterload is directly related to
109 the stiffness of these posts. To enable magnetic afterload tuning, some of the posts need to be
110 magnetically responsive.
111
112 1.1.1. Acquire 24-well plate compatible racks of silicone posts (dimensions given in
113 **Supplementary Figure 1**). The racks used in this study were produced by a commercial silicone
114 goods supplier according to these dimensions using silicone with a shore hardness of 40.
115
116 1.1.2. Determine the polarity of the post magnets (e.g., d = 0.5 mm, h = 2.0 mm; see **Table of**
117 **Materials**) by placing them on a larger permanent magnet.
118
119 1.1.3. Keeping a fixed polarity, lubricate the magnets with water and insert them, one at a time,
120 into the outermost posts of the silicone racks.
121
122 NOTE: If you attempt to insert more than one magnet at a time, the additional resistance will
123 make it more difficult to push the magnets to the bottom of the post.
124
125 1.1.4. Use a blunted piece of stainless-steel dental wire (d ≈ 0.4 mm, see **Table of Materials**) to
126 carefully push them to the bottom of the hollow post cavity. You can stack up to five magnets in
127 each post.
128
129 1.1.5. Use (round-nose) pliers to bend stainless steel dental wire (d ≈ 0.4 mm, see **Table of**
130 **Materials**) into braces 11.25 mm wide and 15 mm long. Use wire cutters to cut the braces and a
131 file to smooth the cutting surface. To ensure the correct dimensions are achieved, one can use a
132 self-made jig to aid in the wire bending.

133

134 NOTE: Post immobilization can also be achieved by braces made from other materials, as long as
135 they are non-magnetic and rigid.

136

137 1.1.6. Lubricate the braces with water and insert them into the silicone rack, fixing the second-
138 and third- to outermost post in the process (see **Figure 1** for complete silicone rack setup).

139

140 NOTE: Optionally, in order to adapt the baseline stiffness of the control posts to match that of
141 the magnetically responsive posts, fragments of styrene round rod (see **Table of Materials**) can
142 be inserted into the empty posts (those without a brace or magnet).

143

144 1.1.7. Let the racks stand for 1–2 days to allow for any remaining water to air dry.

145

146 1.1.8. When the posts are dry, seal the holes at the top of the hollow silicone posts containing
147 the magnets using a drop of silicone glue.

148

149 1.2. The afterload tuning device

150

151 NOTE: As the magnets in the afterload tuning device are moved towards or away from those in
152 the silicone posts, the attractive magnetic forces increase or decrease accordingly, resulting in
153 altered stiffness of the silicone posts. This movement is achieved using a piezoelectric stage. Due
154 to the prototypical nature of the afterload tuning device, detailed step-by-step instructions on
155 how to replicate it will not be provided. Instead, generalized guidelines for constructing a similar
156 afterload tuning device are detailed herein.

157

158 1.2.1. Obtain a highly precise piezoelectric linear motor to enable the vertical translation of the
159 magnet plate towards and away from the EHTs (see **Table of Materials**).

160

161 NOTE: It is highly suggested that this motor be fitted with a linear encoder to correct for stage
162 positioning.

163

164 1.2.2. Position a set of permanent magnets within a non-magnetic holder such that they are
165 axially aligned with the post magnets when placed directly below them. Here, large cylindrical
166 magnets (d = 13 mm, h = 14 mm; see **Table of Materials**) were press-fit within an acrylic plastic
167 plate ("magnet plate").

168

169 1.2.3. Attach the magnet holder to the piezoelectric stage using a non-magnetic material. This
170 can be achieved using an L-shaped piece of aluminum (see **Figure 2**).

171

172 1.2.4. Construct a frame that can house the components of the afterload tuning device. At a
173 minimum, this structure should have a location on which to vertically mount the piezoelectric
174 stage, as well as a rigid frame on which to place the 24-well plate.

175

176 NOTE: It is suggested that the location of this mount be modifiable in the horizontal plane in
177 order to allow for adjustments in axial alignment between the two sets of magnets. A system of
178 mechanical drives was used to achieve this maneuverability in the presented system (**Figure 3**).
179 The afterload tuning device described here was designed to be compatible with the EHT
180 contractility analysis system (see **Table of Materials**). As such, its dimensions were restricted to
181 29 cm in width, 29 cm in depth, and 16 cm in height to fit within this system.

183 1.2.5. To enable visual analysis of the tissues, install a light source within the afterload tuning
184 device. Here, an array of LEDs was employed (**Figure 4**) to illuminate the EHTs from below (**Figure
185 5**).

187 1.3. Calibrating the afterload tuning system

189 NOTE: In order to precisely augment EHT afterload to the desired value, the relationship between
190 magnet spacing and the resulting post stiffness will need to be determined.

192 1.3.1. Measure the closest (d_{min}) and farthest (d_{max}) magnet spacing possible in your setup. These
193 distances will dictate the maximum and minimum achievable afterloads.

195 NOTE: The bottom of the culture plate will prevent direct contact between the magnet plate and
196 the magnetically responsive silicone posts.

198 1.3.2. Produce a range of non-magnetic weights and mount them on string to serve as test loads.

200 1.3.3. Determine the weights of the test loads using a fine scale and label them according to this
201 weight. Here, six different acrylic glass weights ranging from 30 mg to 200 mg were used.

203 NOTE: Select weights that are heavy enough to bend the post, but not so heavy that they bend
204 the post more than a few millimeters. Using a larger number of test loads ensures that the
205 calibration is more precise but it will also be more time-consuming.

207 1.3.4. Mount one of the silicone racks vertically (using non-magnetic materials), such that the
208 magnetically responsive silicone posts are oriented horizontally.

210 1.3.5. Mount one of the plate magnets (the "calibration magnet") on a horizontally traveling
211 linear stage such that it is axially aligned with the magnetically responsive post.

213 1.3.6. Position the calibration magnet a defined distance from the magnetically responsive
214 silicone post using the horizontal stage (preferably, start at a distance equal to the maximum
215 magnet spacing achievable by the afterload tuning device).

217 1.3.7. Place a camera (for an example, see **Table of Materials**) to the side of this set-up in order
218 to be able to optically record the post's deflection under the influence of the test loads.

219

220 NOTE: It is suggested that the user employ a camera with a resolution of at least 2 megapixels to
221 ensure accurate determination of post deflection.

223 1.3.8. Take a picture of the post in the absence of any weights to use as a reference for the post's
224 "neutral" position.

226 1.3.9. Without changing the camera's perspective, attach one of the loads to the very end of the
227 silicone post and take a picture of the post bending under the influence of the weight.

229 1.3.10. Repeat this measurement for all of the weights.

231 1.3.11. Optically determine the deflection of the silicone post caused by the gravitational force
232 of each weight.

234 1.3.12. Graph the deflection of the silicone post (x, on the x-axis) against the gravitational force
235 of each test weight (mg, on the y-axis). This should yield a linear relationship between force and
236 deflection.

238 NOTE: If the data is non-linear, this may indicate that the post is outside its linear range of
239 deflection, i.e., the utilized weights were too heavy.

241 1.3.13. Plot a linear regression function passing through (0,0) and the acquired data (see **Figure
242 6A** for examples). The slope of this function ($mg = kx$) is the stiffness k of the magnetically
243 responsive silicone post at the tested magnet spacing.

245 1.3.14. Repeat these steps at several spacings between d_{max} and d_{min}. Here, deflections at nine
246 different magnet positions ranging from ~31 mm to ~5 mm were analyzed.

248 1.3.15. Determine the base stiffness of the magnetically responsive silicone post in the absence
249 of the calibration magnet using the same technique.

251 1.3.16. Also determine the stiffness of a mobile, non-magnetically responsive control post using
252 the same technique.

254 1.3.17. Plot the resulting k values against the respective magnet distances. This should yield a
255 negative exponential relationship.

257 1.3.18. Plot a regression function through these values. For example, use **Non-linear fit | One-
258 phase decay** function in the analysis software (see the **Table of Materials**). This regression
259 function describes the relationship between magnet spacing and afterload (see **Figure 6B** for an
260 example).

262 **2. EHT generation and culture**

264

265 NOTE: EHT generation and culture have been described in great detail in another article[25].
266 Therefore, we will only cover these aspects briefly in our protocol. Please carry out the following
267 steps under sterile conditions, adhering to good cell culture practices.

268

269 2.1. EHT generation

270

271 2.1.1. Immerse the previously prepared silicone racks in a container filled with 70% ethanol for
272 at least 20 min.

273

274 CAUTION: Do not autoclave the afterload-adjustable silicone posts to sterilize them as high
275 temperatures can damage the permanent magnets.

276

277 2.1.2. Bring this container into the biosafety cabinet, rinse the racks 2x with sterile water, and let
278 them air dry.

279

280 NOTE: To reduce the likelihood of contamination, this process should be carried out in the same
281 biosafety cabinet that will later be used to cast the EHTs.

282

283 2.1.3. Acquire (and thaw if necessary) neonatal rat heart ventricular cells or hiPSC (human
284 induced pluripotent stem cell)-derived cardiomyocytes (also commercially available) and prepare
285 the EHT reconstitution mix according to **Table 1**.

286

287 2.1.4. Pipet 1.5 mL of warm 2% agarose solution into the leftmost 4 wells of a 24-well culture
288 plate and immediately insert a polytetrafluoroethylene (PTFE) spacer (see **Table of Materials**)
289 into the liquid agarose solution.

290

291 2.1.5. Repeat the previous step for the remaining 20 wells within the culture plate.

292

293 2.1.6. After allowing the agarose to solidify for ~10 min, carefully remove the PTFE spacers.

294

295 NOTE: The agarose turns turbid when it has solidified.

296

297 2.1.7. Insert the posts of the magnetically sensitive silicone racks into the agarose voids produced
298 by the PTFE spacers.

299

300 2.1.8. Pipet 100 μL of the reconstitution mix into a 3 μL aliquot of 100 mU/L thrombin solution.
301 Pipette up and down twice to mix and quickly transfer the mixture into the void within the first
302 agarose mold on the culture plate.

303

304 2.1.9. Repeat the previous step for the remaining 23 molds, using a new pipet tip for every EHT.

305

306 NOTE: Gently mix the constitution mix every 6–8 EHTs in order to prevent cell sedimentation.

307

308 2.1.10. Store the 24-well plate in an incubator (37 °C, 7% CO_2, 40% O_2) for 90 min. In the
309 meantime, prepare the EHT medium by supplementing Dulbecco's modified Eagle medium
310 (DMEM) with 10% horse serum, 1% penicillin/streptomycin, 10 µg/mL insulin and 33 µg/mL
311 aprotinin.
312
313 2.1.11. Add 500 µL of warm EHT medium to each well.
314
315 2.1.12. Store the 24-well plate in an incubator (37 °C, 7% CO_2, 40% O_2) for 30 min. During this
316 time, prepare a second 24-well plate with 1.5 mL of EHT medium in each well and place it in the
317 incubator.
318
319 2.1.13. Carefully remove the magnet-sensitive silicone racks with the freshly cast EHTs on them
320 from the agarose molds and transfer them to the second 24-well plate.
321
322 2.2. EHT culture
323
324 NOTE: Following tissue casting, change medium three times per week: on Monday, Wednesdays,
325 and Fridays.
326
327 2.2.1. For a medium change, pipet 1.5 mL of fresh EHT medium per well into a new 24-well
328 culture plate and place this plate within the incubator at 37 °C, 7% CO_2, and 40% O_2 for at least
329 30 min.
330
331 2.2.2. Transfer the silicone racks from the old 24-well plate to the new plate under a cell culture
332 hood.
333
334 2.2.3. Store the closed EHT plates in an incubator at 37 °C, 7% CO_2, and 40% O_2.
335
336 **3. Afterload modification experiments**
337
338 NOTE: The following protocol steps are specific to the piezoelectric motor and optical
339 contractility analysis platform listed in the **Table of Materials**.
340
341 3.1. Preparing the afterload tuning device for experiments
342
343 3.1.1. To measure the effects of afterload manipulations on EHT contractility, disconnect and
344 remove the lighting system from the innermost compartment of the optical contractility analysis
345 platform and insert the afterload tuning device including the light source.
346
347 3.1.2. Install the stage motion control software (see **Table of Materials**) on the computer that
348 will be used to run the afterload tuning device.
349

350 3.1.3. Connect the piezoelectric stage motor to the motion controller (see **Table of Materials**),
351 and the motion controller to the computer. Make sure the motion controller is also connected
352 to a power source.
353
354 NOTE: There are two lights on the face of the motion controller. Upon connecting to power, both
355 lights flash red for a few seconds. During operation, the upper light remains green while the lower
356 one should only turn red if an error occurs.
357
358 3.1.4. Place an empty 24-well culture plate on the plate mount at the top of the afterload tuning
359 device.
360
361 3.1.5. Optically align the empty culture plate with the magnet plate below using the XY
362 mechanical drive system attached to the mount.
363
364 3.2. Operating the afterload-tuning device
365
366 3.2.1. Start the motion controller platform software.
367
368 3.2.2. Connect the software to the piezo stage motor by selecting the port designated as the
369 stage port during installation of the motion control software and then click the **open port** button.
370
371 NOTE: After completing this step, the port should be designated as "open" and appear in a green
372 box.
373
374 3.2.3. Go to the **System** panel. Select **Open Loop** in the **Loop** dropdown menu.
375
376 3.2.4. Manually move the magnet plate to its highest position, i.e., the closest possible magnet
377 spacing d_{min}. The magnet plate should make contact with the culture plate mount.
378
379 3.2.5. Go to the **Motion** panel. Click the **Zero** button to reset the current position of the piezo
380 stage to 0 mm.
381
382 3.2.6. Manually move the magnet plate to its lowest possible position. Write down the encoder
383 position (indicated in the **Motion** panel by **Enc**) to determine the range of motion for the
384 piezoelectric stage motor.
385
386 3.2.7. Set the **Travel Limits** in the **System** panel to values within the range of motion determined
387 in the previous step. This prevents the magnet plate from bumping into the culture plate or the
388 bottom of the afterload tuning device.
389
390 3.2.8. Once again, move the magnet plate to its highest position and click the **Zero** button.
391
392 3.2.9. Go to the system panel and change the feedback loop mode to **Closed Loop**. Doing this
393 ensures that the stage will correct for any errors in its positioning.

394

395 3.2.10. Click the **Save** button in the **Save Parameters** box to store these settings in the system.

396

397 3.2.11. Place a 24-well culture plate containing EHTs on magnetically responsive silicone racks on
398 the culture plate mount.

399

400 3.2.12. To calculate the magnet spacing necessary to achieve a desired afterload, solve the
401 nonlinear regression function from step 1.3.19 for the magnet spacing parameter d. For example,
402 if the equation is: $d = -4.95 \times \ln\left(\frac{k-2.90}{24.34}\right)$, d being the magnet spacing (in mm) necessary to
403 achieve the desired afterload k in mN/mm, a magnet spacing of 12.12 mm would be necessary
404 to achieve an afterload of 5 mN/mm.

405

406 3.2.13. Subtract d_{min} from the calculated magnet spacing d. The result is the distance the magnet
407 plate has to travel from its **Zero** position to achieve the desired afterload.

408

409 3.2.14. Type this value into the **Target Position 1** input field in the **Motion** panel and click **Go** to
410 adjust the EHTs' afterload to the calculated value.

411

412 3.3. Optional: Programming the stage for an interval afterload regimen

413

414 NOTE: The previous section describes how to program the stage to move to and stay at a single
415 position. However, it is also possible to chain different commands together into a program to
416 achieve an automatically executed sequence of motions, which may be repeated on a continuous
417 loop. For more detailed instructions regarding the motion controller platform software, consult
418 the operation manual provided by the stage manufacturer.

419

420 3.3.1. After setting up the afterload tuning device as described in the previous section, open the
421 **Command** panel. Type the command *1PGM1* and press **Enter** to start recording a program.

422

423 3.3.2. To create a program which, for example, will cause the piezoelectric stage to move down
424 30 mm from the **Zero** position (away from the EHTs) and return after 40 s, enter the following
425 chain of commands: *1MVA30 → 1WST → 1WTM40000 → 1MVA0 → 1WST*

426

427 3.3.3. Use the command *1END* to conclude recording a program and save it.

428

429 3.3.4. Use the command *1EXC1* to execute the recorded program.

430

431 3.3.5. To keep the program running on a continuous loop, enter *1PGL1*, followed by the *1EXC1*
432 command.

433

434 3.3.6. To terminate a looping program, enter the command *1EST*.

435

436 NOTE: **Table 2** contains some useful commands for afterload modification experiments. A

437 complete list of available commands for this system can be found in the reference manual for
438 the modular motion control system.
439
440 **REPRESENTATIVE RESULTS:**
441
442 **Magnet post stiffness quantification**
443 A horizontally oriented magnetically responsive silicone post was mounted in a fixed position,
444 and an axially aligned calibration magnet was placed at several defined distances ("magnet
445 spacings") from this post. Test loads of known weight were suspended from the end of the
446 silicone post, causing the post to bend. This deflection was quantified optically. A linear
447 relationship between the gravitational force of the test load and resulting post deflection was
448 observed at all magnet spacings (**Figure 6A**). The values of stiffness derived from these linear
449 relationships followed a negative exponential trend with increasing magnet spacing (**Figure 6B**).
450
451 **Stepwise afterload increase**
452 Control and magnetically responsive EHTs (MR-EHTs) produced from rat hearts were cultured in
453 the absence of magnetic afterload (0.6 mN/mm for control tissues and 0.91 mN/mm for MR-
454 EHTs) until a plateau in contractile force was reached. On this day (24 days following EHT casting),
455 MR-EHTs and control EHTs had similar mean forces (0.29 mN versus 0.22 mN). Over the next
456 week, the afterload exerted on MR-EHTs was incrementally increased from 0.91 to 6.85 mN/mm,
457 while afterload for control EHTs remained constant. Mean contractile force increased with
458 increasing afterload up to 0.95 mN, which marks more than a 3-fold increase in force compared
459 to the average value (0.29 mN) measured for control EHTs (**Figure 7A**). Post deflection, on the
460 other hand, decreased compared to control tissues. On the last day of culture, the mean
461 deflection measured for MR-EHTs was only 0.11 mm compared to 0.48 mm for control EHTs
462 (**Figure 7B**). From day 27 on, force production rate and force decay rate were higher in MR-EHTs
463 than in control EHTs while there was only a transient increase in work over days 25–28
464 (**Supplementary Figure 2**).
465
466 **Interval afterload regimen**
467 Rat EHTs on magnetically responsive silicone posts (MR-EHTs) were cultured at a minimal
468 afterload of 0.91 mN/mm until a plateau in contractile force was reached. From this day (17 days
469 following EHT casting) onward, MR-EHTs underwent a 7-day afterload regimen which exposed
470 the EHTs to cycles of afterloads alternating between 0.91 and 6.85 mN/mm (**Figure 8A**). The
471 afterload of control EHTs was kept constant at 0.60 mN/mm over the entire duration of culture.
472 Following this intervention, average forces for MR-EHTs increased by 12.0% compared to day 17,
473 while those measured for control EHTs only increased by 1.5% over the same time frame (**Figure
474 8B**). However, these differences were not statistically significant. Moreover, no significant
475 differences in force production rate, force decay rate and contractile work were measured
476 (**Supplementary Figure 3**). This implies that the selected afterload regimen was not an efficient
477 means of increasing EHT contractility.
478
479 **FIGURE AND TABLE LEGENDS:**
480

Figure 1: Assembled magnetically responsive silicone racks. (**A**) Orthogonal view and (**B**) sectional view of assembled magnetically responsive silicone racks containing five magnets.

Figure 2: Magnet plate. Photograph of the magnet plate and its attachment bracket.

Figure 3: Mechanical drive system. Photograph showing the system of mechanical drives used to adjust the horizontal position of the 24-well plate with respect to the magnet plate.

Figure 4: LED plate. Photograph of the LED plate used to illuminate EHTs for optical contractility analysis.

Figure 5: Fully assembled afterload tuning device. Photograph of the fully assembled afterload tuning device including the LED plate.

Figure 6: Optical determination of post stiffness. (**A**) The deflection of a magnetically responsive silicone post in the presence of an external calibration magnet and under the influence of five test weights was assessed at nine determined magnet spacings (five shown as examples). (**B**) Determined relationship between magnet spacing and post stiffness.

Figure 7: Contractile response of EHTs to a stepwise increase in afterload. Contractile measurements of control EHTs (black line) and EHTs cultured on magnetically responsive posts (MR-EHTs; blue line) over a culture period of 31 days. (**A**) MR-EHTs had slightly higher average contractile forces than control EHTs under baseline conditions. From day 25 on, however, this difference was amplified with increasing afterload. (**B**) Post deflection was similar between both groups until day 27. Past afterload values of 3.5 mN/mm, post deflection for MR-EHTs dropped substantially. Here, n = 10 MR-EHTs and n = 10 control EHTs were analyzed by fitting a mixed model (REML = restricted maximum likelihood) and Sidak's multiple comparison test. The error bars in graphs represent standard error of the mean, ** $p < 0.01$, *** $p < 0.001$.

Figure 8: Contractile response of EHTs to an interval afterload protocol. The contractile behavior of magnetically responsive EHTs under the influence of a fluctuating regimen of afterload was observed. (**A**) The afterload regimen, which was initiated on day 17 (d17), exposed the MR-EHTs to 40 s intervals of minimal afterload (0.91 mM/mm) followed by 40 s intervals of maximal afterload (6.85 mN/mm) for 7 days. (**B**) MR-EHTs (blue bars) showed a trend towards increasing forces during the interval afterload protocol, while the forces measured for control EHTs (black bars) remained relatively unchanged. For these experiments, n = 10 EHTs were analyzed per group and this data was statistically compared using a 2-way ANOVA and Sidak's multiple comparison test. Error bars in graphs represent standard error of the mean.

Table 1: Reconstitution mix for generating EHTs.

Table 2: Useful commands for afterload tuning experiments.

Supplementary Figure 1: Dimensions of silicone racks. (**A**) Top view, (**B**) sectional side view, and

525   (**C**) detailed post view of the silicone racks used for these studies.

526

527   **Supplementary Figure 2: Additional contractile parameters for stepwise afterload increase.**
528   Contractile measurements of control EHTs (black line) and EHTs cultured on magnetically
529   responsive posts (MR-EHTs; blue line) over a culture period of 31 days. (**A**) MR-EHTs had a
530   significantly higher force production rate than control EHTs from day 27 on. (**B**) The rate of force
531   decay was also significantly greater in MR-EHTs than in control from day 27 onward. (**C**) While
532   contractile work measured in control EHTs gradually increased over the entire period of culture,
533   the contractile work produced by MR-EHTs peaked on day 26 and dropped thereafter to levels
534   below control. Yet, work in MR-EHTs was never significantly higher than that in control EHTs.
535   Here, n = 10 MR-EHTs and n = 10 control EHTs were analyzed by fitting a mixed model (REML =
536   restricted maximum likelihood) and Sidak's multiple comparison test. The error bars in graphs
537   represent standard error of the mean, * $p < 0.05$, *** $p < 0.001$.

538

539   **Supplementary Figure 3: Additional contractile parameters for interval afterload protocol.** The
540   contractile behavior of magnetically responsive EHTs (MR-EHTs) under the influence of a
541   fluctuating regimen of afterload was observed. (**A**) During the interval afterload protocol, MR
542   EHTs (blue bars) initially showed a trend towards higher force production rates compared to
543   control EHTs (black bars), but these differences were not significant and diminished towards the
544   end of the experiment. (**B**) Force decay rates measured in MR-EHTs and control EHTs were
545   statistically similar throughout the interval afterload protocol. (**C**) Contractile work measured for
546   MR-EHTs increased during the first days of the afterload interval protocol but decreased on the
547   last day. The contractile work measured for control EHTs did not noticeably change during this
548   period of time. Work in MR-EHTs was never significantly higher than work in control EHTs. For
549   these experiments, n = 10 EHTs per group were analyzed by 2-way ANOVA and Sidak's multiple
550   comparison test. Error bars in graphs represent standard error of the mean.

551

552   **DISCUSSION:**
553   The protocol outlined herein describes a new technique for magnetically altering afterload in
554   engineered heart tissues. This technique relies upon the use of a piezoelectric stage to translate
555   a plate of strong magnets towards and away from magnetically responsive racks of silicone posts.
556   The closer the two sets of magnets, the stronger the afterload experienced by the EHTs cultured
557   on them.

558

559   There are several steps that are critical to the successful production and use of this system. While
560   fabricating the magnetically responsive silicone racks, it is crucially important to ensure that all
561   of the magnets within the posts are oriented with the same polarity. If a magnet is placed in the
562   reverse orientation, it will serve to weaken rather than augment the strength of the magnetic
563   field. Similarly, this polarity should match that of all the magnets within the magnet plate, else
564   the two sets of magnets will repel, rather than attract one another. Additionally, where possible,
565   refrain from using magnetic materials in the construction of the afterload adjustment device, as
566   they can interfere with the magnetic field. Aluminum is suggested as a primary construction
567   material for this reason. Similarly, if using a piezoelectric stage other than the one listed in the
568   **Table of Materials**, ensure that it is resistant to magnetic fields and standard cell culture

569   conditions (e.g., 37 °C, 100% humidity, and high CO_2 and O_2-concentrations). Lastly, keep in mind
570   that most piezoelectric linear stages are meant to be mounted horizontally, as they tend to have
571   a low load capacity. As such, if the weight of the magnet plate exceeds this load capacity, a
572   counterweight should be used to unload the motor.
573
574   Despite best practices, it is quite difficult to keep the encoder surface pristine. When this occurs,
575   the stage will stop moving before reaching the target position when running in closed-loop mode.
576   The motion controller's red LED will flash, additionally the motion controller software will display
577   a "No encoder detected"-error message. To remedy this, the user should clean the surface of the
578   encoder with a lint-free piece of cloth soaked in isopropyl alcohol and let it air dry.
579
580   This protocol demonstrates the steps taken by our lab to produce and implement this system.
581   However, several of these steps could be achieved by different means. For example, one could
582   use a force transducer, rather than optical means, to confirm the relationship between magnet
583   spacing and post stiffness. Additionally, custom posts could be designed and fabricated with
584   embedded magnets and braces. However, we have found that precise positioning of these
585   objects is easier to accomplish manually. To fine-tune the range of afterloads applicable by this
586   system, these posts can be manufactured with differing basal stiffnesses or with a different
587   number of magnets. Though, using too many magnets will impede post bending. Alternatively,
588   this can also be achieved by adjusting the size and strength of the magnets within the magnet
589   plate. Larger and stronger magnets will yield higher afterloads.
590
591   There are several limitations to this method that could be improved upon in future versions of
592   this system. Namely, the range of applicable afterloads is physically limited by the maximum and
593   minimum spacing between the post magnets and plate magnets. Ideally, the posts used for this
594   system would place the tissues as close to the base of the tissue culture dish as possible, without
595   directly allowing the tissue to touch the bottom of the plate. However, the posts used in these
596   studies were commercially made prior to the development of this system, so the lengths of the
597   posts were not optimized for this platform. Similarly, since the EHT contractility analysis system
598   was constructed prior to this system, it was not designed to allow for electrical cords in or out of
599   the measurement space. As such, the presence of these cords resulted in a small air gap, which
600   allowed for gases to slowly leak out of the inner chamber. This could be ameliorated by adjusting
601   gas flow rates accordingly. However, ideally, a future embodiment of this system would have
602   insulated exit and entry points for these cords. Should one wish to perform these experiments in
603   the absence of the EHT contractility analysis system, the afterload tuning platform can instead
604   be placed within an incubator. Though, the system in its entirety will only fit within a standard
605   incubator if one or more of the shelves are removed, rendering this space unavailable for other
606   cell and or tissue culture purposes. To optically observe the tissues in either environment, lights
607   will be necessary. The LED lights used for this system were found to give off a substantial amount
608   of heat. If left on for long periods, this heat could potentially damage the tissues. As such, for
609   these studies, the lights were only used for short periods while assessing the contractility of the
610   tissues. However, should one desire to consistently observe the tissues, the lighting system will
611   have to be optimized for these purposes.
612

Afterload has been previously studied in EHT models[16,23]. However, these works presented techniques that were only able to achieve a singular static increase in load. Alternatively, this work demonstrated how a magnetics-based platform can be used to fine-tune and temporally regulate afterload in EHTs. The results from two separate sets of experiments were used to exemplify the wide range of afterload regimens that can be applied to EHTs using this device. Intended future applications of this system include studies on the effect of the applied afterload regimen (dose and duration) on both tissue maturation and pathological remodeling.

DISCLOSURES:
TE and MNH are co-founders of EHT Technologies GmbH. All other authors have nothing to disclose.

REFERENCES:
1   Zipes, D. P., Libby, P., Bonow, R. O., Mann, D. L., Tomaselli, G. F. *Braunwald's Heart Disease: A Textbook of Cardiovascular Medicine*. 11th edn, (Elsevier, 2018).
2   McCain, M. L., Yuan, H., Pasqualini, F. S., Campbell, P. H., Parker, K. K. Matrix elasticity regulates the optimal cardiac myocyte shape for contractility. *American Journal of Physiology-Heart and Circulatory Physiology.* **306** (11), H1525-1539, doi:10.1152/ajpheart.00799.2013 (2014).
3   de Groot, P. C., van Dijk, A., Dijk, E., Hopman, M. T. Preserved cardiac function after chronic spinal cord injury. *Archives of Physical Medicine and Rehabilitation.* **87** (9), 1195-1200, doi:10.1016/j.apmr.2006.05.023 (2006).
4   Perhonen, M. A. et al. Cardiac atrophy after bed rest and spaceflight. *Journal of Applied Physiology.* **91** (2), 645-653, doi:10.1152/jappl.2001.91.2.645 (2001).
5   Levy, D., Larson, M. G., Vasan, R. S., Kannel, W. B., Ho, K. K. The progression from hypertension to congestive heart failure. *Journal of the American Medical Association.* **275** (20), 1557-1562, doi:10.1001/jama.1996.03530440037034 (1996).
6   Levy, D. et al. Long-term trends in the incidence of and survival with heart failure. *The New England Journal of Medicine.* **347** (18), 1397-1402, doi:10.1056/NEJMoa020265 (2002).
7   Maggioni, A. P. et al. EURObservational Research Programme: regional differences and 1-year follow-up results of the Heart Failure Pilot Survey (ESC-HF Pilot). *European Journal of Heart Failure.* **15** (7), 808-817, doi:10.1093/eurjhf/hft050 (2013).
8   Mozaffarian, D. et al. Heart disease and stroke statistics--2015 update: a report from the American Heart Association. *Circulation.* **131** (4), e29-322, doi:10.1161/CIR.0000000000000152 (2015).
9   Klautz, R. J., Teitel, D. F., Steendijk, P., van Bel, F., Baan, J. Interaction between afterload and contractility in the newborn heart: evidence of homeometric autoregulation in the intact

657 circulation. *Journal of the American College of Cardiology.* **25** (6), 1428-1435, doi:10.1016/0735-
658 1097(94)00562-5 (1995).

10 Liedtke, A. J., Pasternac, A., Sonnenblick, E. H., Gorlin, R. Changes in canine ventricular
660 dimensions with acute changes in preload and afterload. *The American Journal of Physiology.* **223**
661 (4), 820-827, doi:10.1152/ajplegacy.1972.223.4.820 (1972).

11 Toischer, K. et al. Differential cardiac remodeling in preload versus afterload. *Circulation.*
663 **122** (10), 993-1003, doi:10.1161/CIRCULATIONAHA.110.943431 (2010).

12 Zhang, H. et al. Cellular Hypertrophy and Increased Susceptibility to Spontaneous
665 Calcium-Release of Rat Left Atrial Myocytes Due to Elevated Afterload. *PloS one.* **10** (12),
666 e0144309, doi:10.1371/journal.pone.0144309 (2015).

13 Hori, M. et al. Loading sequence is a major determinant of afterload-dependent relaxation
668 in intact canine heart. *The American Journal of Physiology.* **249** (4 Pt 2), H747-754,
669 doi:10.1152/ajpheart.1985.249.4.H747 (1985).

14 Schotola, H. et al. The contractile adaption to preload depends on the amount of
671 afterload. *ESC Heart Failure.* **4** (4), 468-478, doi:10.1002/ehf2.12164 (2017).

15 Sonnenblick, E. H., Downing, S. E. Afterload as a primary determinat of ventricular
673 performance. *The American Journal of Physiology.* **204** 604-610,
674 doi:10.1152/ajplegacy.1963.204.4.604 (1963).

16 Hirt, M. N. et al. Increased afterload induces pathological cardiac hypertrophy: a new in
676 vitro model. *Basic Research in Cardiology.* **107** (6), 307, doi:10.1007/s00395-012-0307-z (2012).

17 Hirt, M. N. et al. Deciphering the microRNA signature of pathological cardiac hypertrophy
678 by engineered heart tissue- and sequencing-technology. *Journal of Molecular and Cellular
679 Cardiology.* **81** 1-9, doi:10.1016/j.yjmcc.2015.01.008 (2015).

18 Dorn, G. W., 2nd. The fuzzy logic of physiological cardiac hypertrophy. *Hypertension.* **49**
681 (5), 962-970, doi:10.1161/HYPERTENSIONAHA.106.079426 (2007).

19 Hill, J. A., Olson, E. N. Cardiac plasticity. *The New England Journal of Medicine.* **358** (13),
683 1370-1380, doi:10.1056/NEJMra072139 (2008).

20 Maillet, M., van Berlo, J. H., Molkentin, J. D. Molecular basis of physiological heart growth:
685 fundamental concepts and new players. *Nature Reviews Molecular Cell Biology.* **14** (1), 38-48,
686 doi:10.1038/nrm3495 (2013).

21 Stenzig, J. et al. DNA methylation in an engineered heart tissue model of cardiac
688 hypertrophy: common signatures and effects of DNA methylation inhibitors. *Basic Research in
689 Cardiology.* **111** (1), 9, doi:10.1007/s00395-015-0528-z (2016).

22 Werner, T. R., Kunze, A. C., Stenzig, J., Eschenhagen, T., Hirt, M. N. Blockade of miR-140-
691 3p prevents functional deterioration in afterload-enhanced engineered heart tissue. *Scientific
692 Reports.* **9** (1), 11494, doi:10.1038/s41598-019-46818-0 (2019).

23 Leonard, A. et al. Afterload promotes maturation of human induced pluripotent stem cell
694 derived cardiomyocytes in engineered heart tissues. *Journal of Molecular and Cellular Cardiology.*
695 **118** 147-158, doi:10.1016/j.yjmcc.2018.03.016 (2018).

24 Rodriguez, M. L., Werner, T. R., Becker, B., Eschenhagen, T., Hirt, M. N. Magnetics-Based
697 Approach for Fine-Tuning Afterload in Engineered Heart Tissues. *ACS Biomaterials Science &
698 Engineering.* **5** (7), 3663-3675, doi:10.1021/acsbiomaterials.8b01568 (2019).

25 Mannhardt, I. et al. Automated Contraction Analysis of Human Engineered Heart Tissue
700 for Cardiac Drug Safety Screening. *Journal of Visualized Experiments: JoVE.* 10.3791/55461 (122),
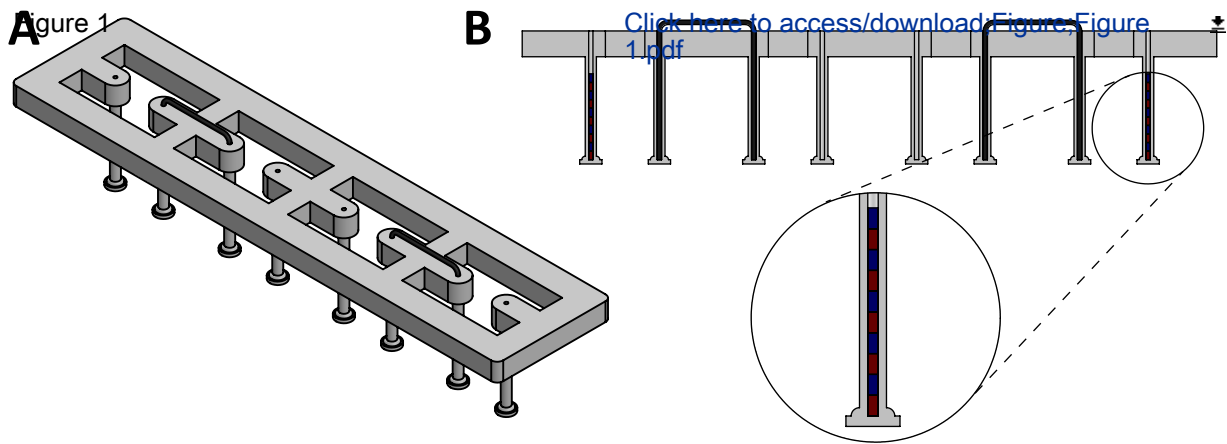
701   doi:10.3791/55461 (2017).
702
703

A

B
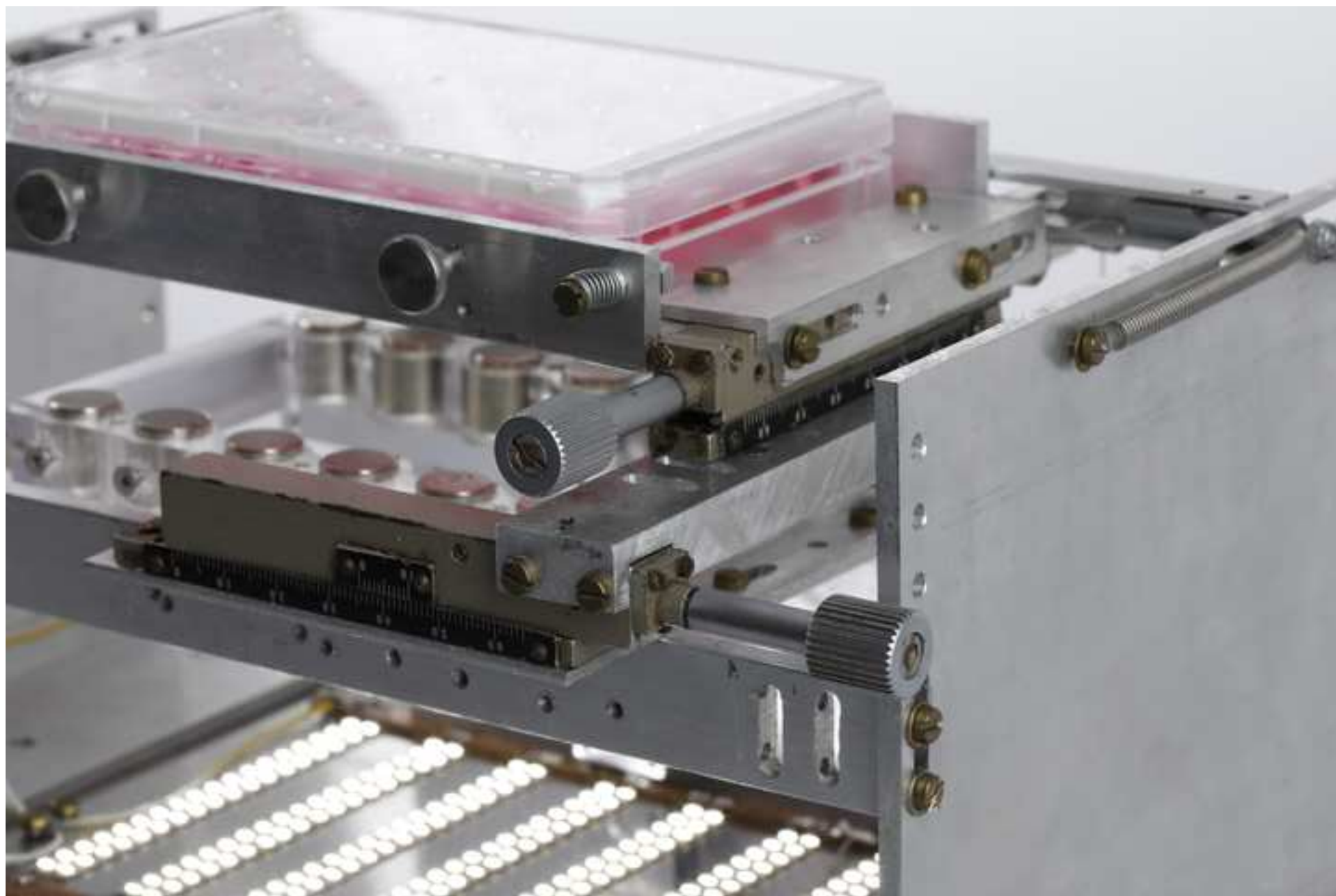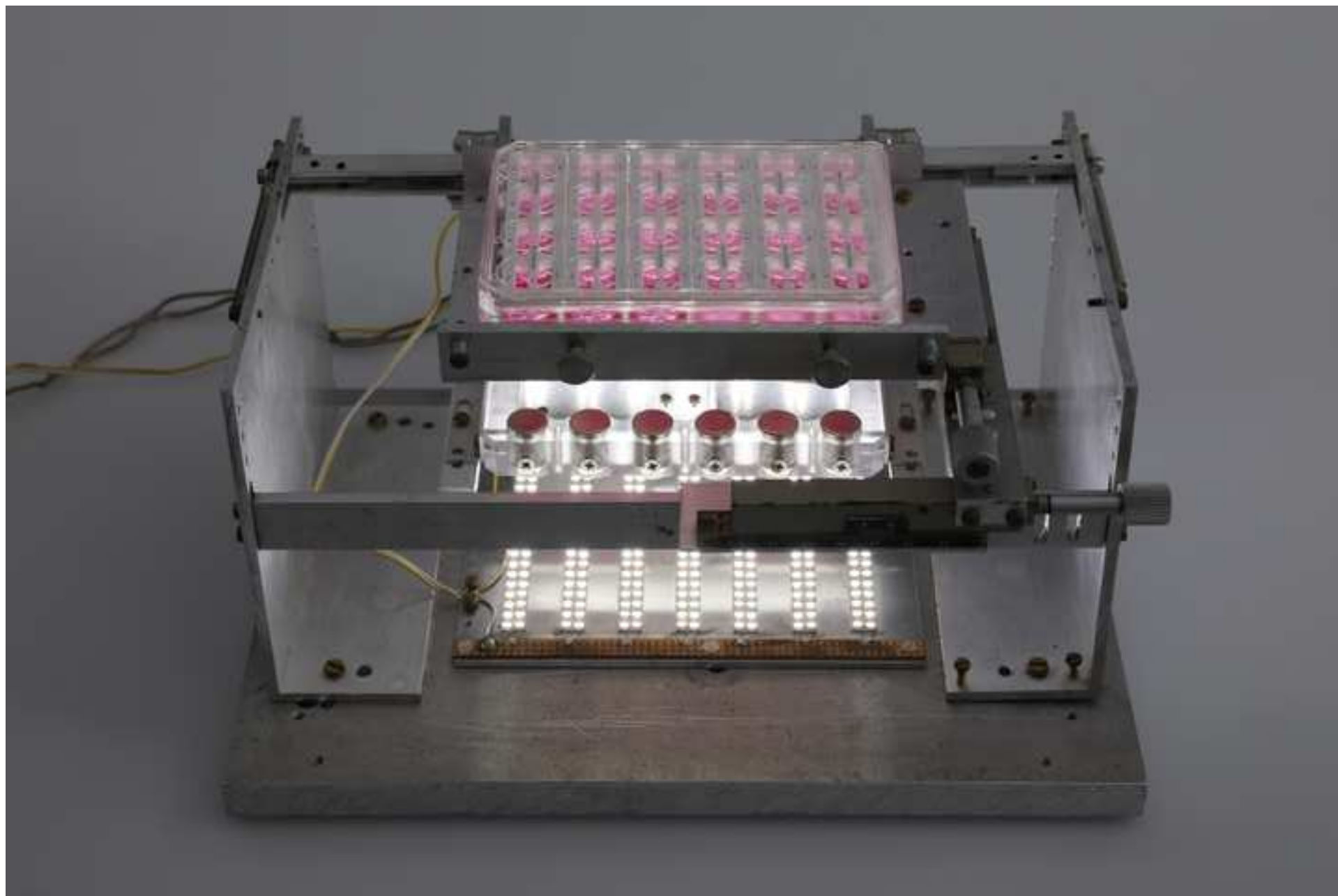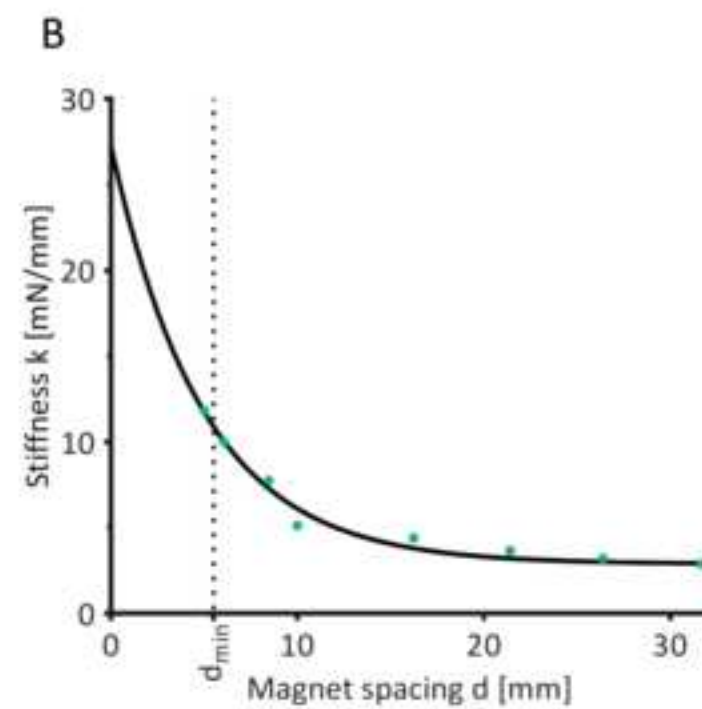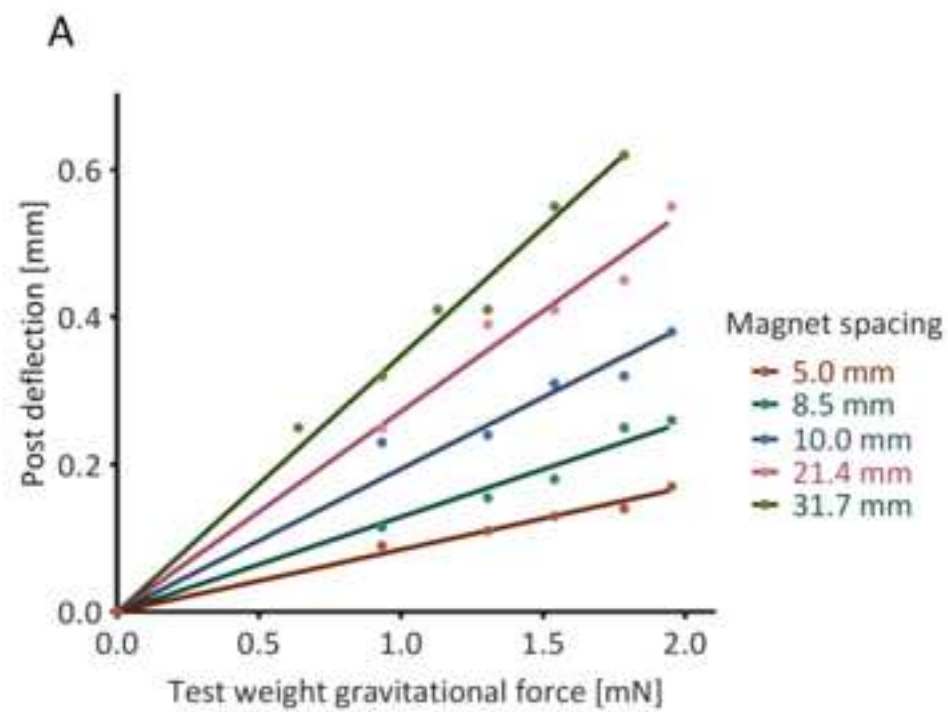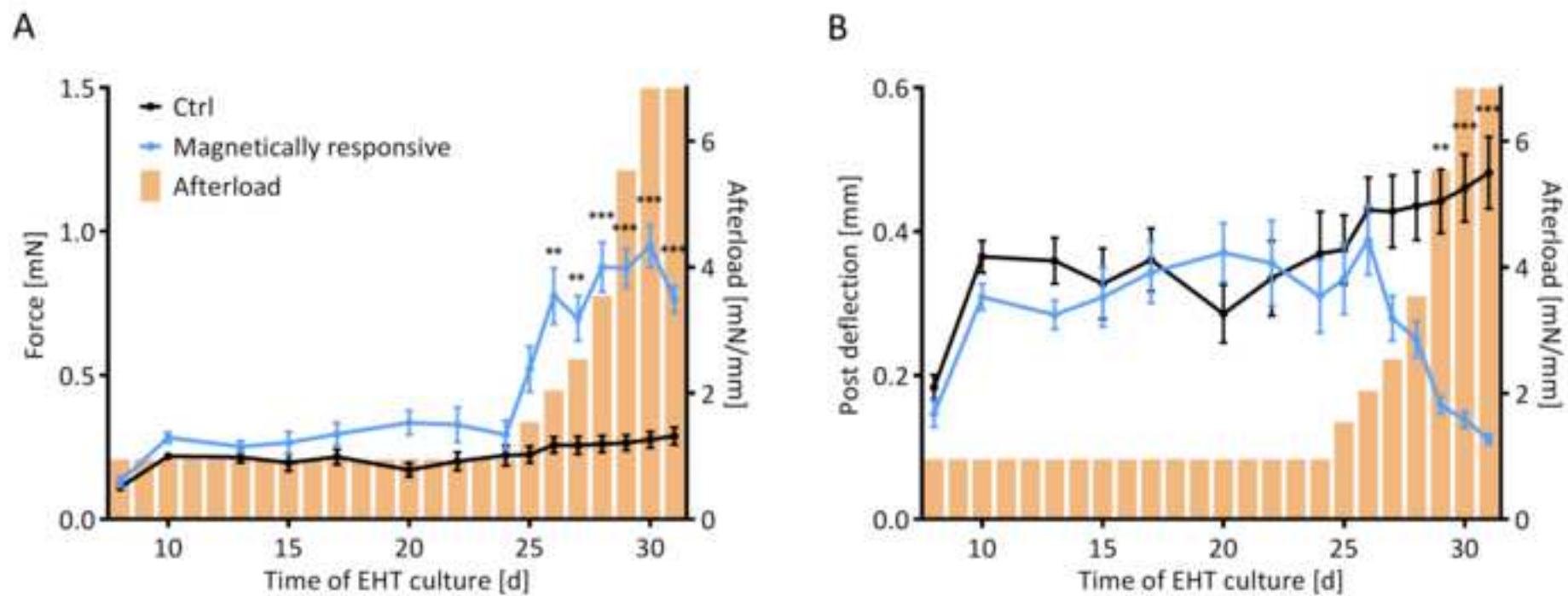
Figure 2

Figure 3

Figure 4

Figure 5

Figure 6

Figure 7

Figure 7

Figure 8
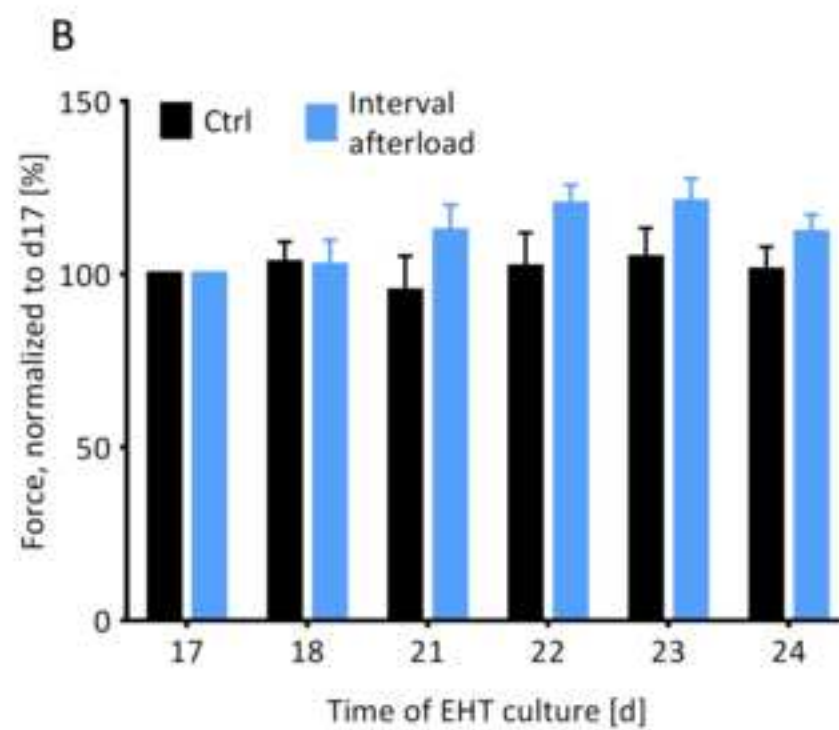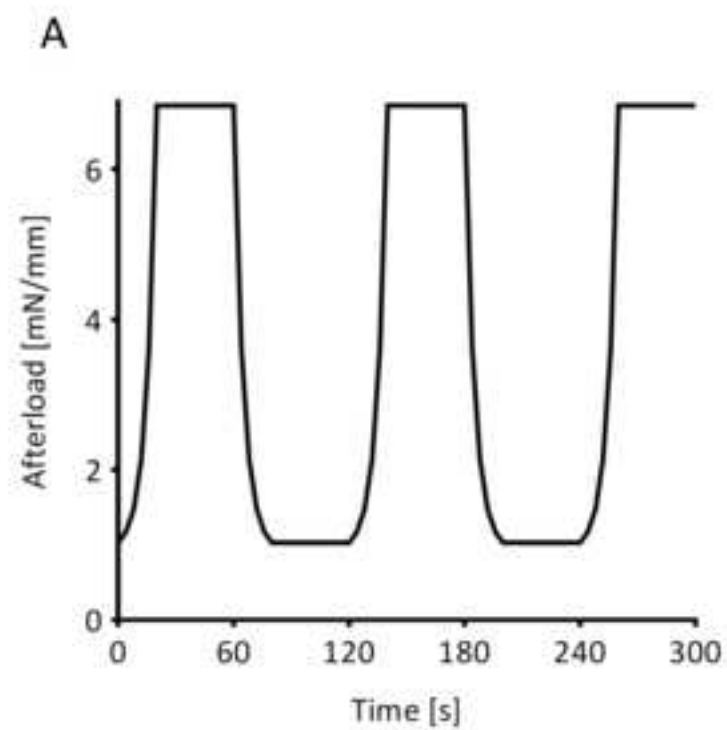
Table 1

1 Rat EHT	24 Rat EHTs (+10%)	1 hiPSC-CM EHT	24 hiPSC-CM EHTs (+10%)	Component
5×10^5	1.3×10^7	1×10^6	2.6×10^7	Cells (either neonatal rat heart ventricular cells or hiPSC-derived cardiomyocytes)
5.57 µL	147 µL	5.57 µL	147 µL	2x DMEM: 20% heat-inactivated horse serum, 20% 10x DMEM, 2% penicillin/streptomycin, 58% aqua ad iniectabilia
2.53 µL	66.8 µL	2.53 µL	66.8 µL	Fibrinogen: 200 mg/mL Fibrinogen dissolved in 0.9% NaCl
-	-	0.1 µL	2.64 µL	Y-27632
ad 100 µL	ad 2640 µL	ad 100 µL	ad 2640 µL	EHT-casting medium: 88% DMEM, 10% heat-inactivated fetal calf serum, 1 % penicillin/streptomycin, 1% L-glutamine

Table 2

Command name	Syntax	Description
Move absolute	1MVA[x]	Stage moves to position [x] in mm
Set velocity	1VEL[x]	Stage movement velocity set to [x] in mm/s
Emergency stop	1EST	Stops any movement
Wait for stop	1WST	Only during program recording; Waits for completion of previous movement command before executing next command
Wait for time period	1WTM[x]	Only during program recording; Waits for time period [x] in ms
Beginn program recording	1PGM[x]	Begin program recording in slot [x]; **Note**: Slot [x] needs to be free
End program recording	1END	End program recording and save program
Erase program	1ERA[x]	Erase program saved in slot [x]
Execute program	1EXC[x]	Execute program saved in slot [x]
Loop program	1PGL[x]	[x]=1 Program loop mode ON [x]=0 Program loop mode turned off
Read and clear errors	1ERR?	Request error report

Table of Materials

Name of Reagent/ Equipment	Company	Catalog Number	Comments/Description
Cylindrical plate magnets	HKCM	9962-55184	h = 14 mm, d = 13 mm
Cylindrical post magnets	HKCM	9962-63571	h = 2 mm, d = 0.5 mm
Dental wire	Ormco	266-1316	d = 0.016 inches (0.406 mm)
GraphPad	GraphPad Software,	version 6.00 for Windows	
Motion control software for piezo motor	Micronix USA		free download on manufacturer homepage
Motion controller for piezo motor	Micronix USA	MMC-100-01000	
Optical contractility analysis platform	EHT technologies	A0001	
Piezoelectric linear motor	Micronix USA	PPS-20-15206	fitted with linear optical encoder, incubator-environment compatible
Styrene Rod	Plastruct	MR-15	d= 0.015 inches (0.381 mm)
USB camera	Reichelt Elektronik	REFLECTA 66142	

UKE
HAMBURG

Institute of Experimental Pharmacology and Toxicology
Center for Experimental Medicine

Thomas Eschenhagen, MD
Director

Martinistraße 52
20246 Hamburg

Marc Hirt, MD, PhD

University Medical Center Hamburg-Eppendorf | Martinistraße 52 | 20246 Hamburg

Institute of Experimental Pharmacology and Toxicology
Center for Experimental Medicine

Alisha D'Souza, PhD
Senior Review Editor
Journal of Visualized Experiments

Building N30
Tel: +49 (0) 40 7410-52180
Fax: +49 (0) 40 7410-54876
m.hirt@uke.de
www.uke.de

Hamburg, November 6, 2019

Response to resubmission request

Dear Dr. D'Souza,

Thank you very much for overseeing the review of our submission "Magnetic Adjustment of Afterload in Engineered Heart Tissues" for publication in the *Journal of Visualized Experiments*. We are pleased that our revisions were well received by the reviewers and appreciate the opportunity to submit a further revised manuscript.

We have addressed the editorial and reviewer comments and believe that the revised manuscript is improved in terms of clarity and completeness. We hope that you now find it suitable for publication.

Sincerely yours,

Marc Hirt

We thank the editor and reviewers for their insightful comments and helpful suggestions, which we believe have greatly improved the quality of our manuscript. Below, we have included a point by point response to each comment. We hope that the following information serves as adequate clarification or resolution of these points.

Editorial Comments

1. Protocol language
   a. Imperative tense

   Where possible, our JoVE protocol has been rewritten in the imperative tense. Those sections that could not be rewritten in this format have been incorporated into notes.

   b. Split up long steps

   Lengthy steps in our protocol have been split into additional steps or simply shortened to enhance the clarity and brevity of our protocol.

2. Protocol highlighting

   We revised the highlighting in order to form a more cohesive narrative.

3. Discussion
   a. Please ensure that the discussion covers the following in detail and in paragraph form (3-6 paragraphs): 1) modifications and troubleshooting, 2) limitations of the technique, 3) significance with respect to existing methods, 4) future applications and 5) critical steps within the protocol.

   In the previous version of the manuscript, we covered each of these topics with the exception of troubleshooting. This section has been added to the revised manuscript.

4. References

   a. Please make sure that your references comply with JoVE instructions for authors.

   We used the official JoVE 2019 Endnote-Style to format references in our manuscript, however, there seem to be small differences between this style and the JoVE instructions for authors. As such, we have added DOI numbers and full journal names to the bibliography.

5. Commercial language

   In accordance with editorial requirements, we have edited our manuscript such that it is absent of commercial language.

Reviewer 1

1. Some parts of the protocol are slightly hard to follow, even with the illustrative figures. Not because the protocol is badly written, but because of the complex nature of the construction/device. I was wondering whether a video of the device in action might help the readers?

   We share the concern of the reviewer that the written instructions are, in certain sections, hard to follow. To address this, we have reselected the portions of the protocol to be filmed such that it covers the more technically challenging portions of the protocol.

2. Typo line 552: (H)owever - h missing

We thank the reviewer for pointing out this oversight. The referenced text has been corrected in the resubmitted version of the manuscript.

3. Figure 7: Last day - is this drop in force caused by the EHTs dying? Has cell viability be looked at. Would be curious to see how sarcomeric structures look in the afterload EHTs compared to control ones (immunofluorescence, e.g. for alpha-actinin)

The main focus of this protocol is to cover the afterload modification-method. As such, we have not investigated what led to this (small) drop in force. However, we have extensively examined the effects of a very strong permanent increase in afterload from 0.95 mN/mm to 11.5 mN/mm (as compared to the gradual increase from 0.9 mN/mm to 6.85 mN/mm in this study). In these previous studies (Hirt et al. 2012 Basic Research in Cardiology [PMID: 23099820] and Hirt et al. 2015 Journal of Molecular and Cellular Cardiology [PMID: 25633833]) we observed a 20% increase in cardiomyocyte death in EHTs subjected to high afterload compared to control EHTs. In addition, fibrotic changes and altered metabolism contributed to the previously described decline in force. We imagine that these events could also be at play here.

For the same reason, we have not stained sarcomeric structures in these tissues. However, preliminary results from experiments utilizing silicone posts of different basal stiffnesses (afterloads) suggest that, over longer periods of time, the average sarcomere length remains unchanged under the range of environmental loads that we are examining. This has also been observed in a similar study from another lab (Leonard et al. 2018 Journal of Molecular and Cellular Cardiology [PMID: 29604261]).

4. Figure 8: if stats have been done and the changes are not significant, this suggests that interval afterload is not a good approach to increase force. If this is the case, this figure and reference to it in the text should be deleted.

We initially hypothesized that tissue contractile force could be increased by exposing the tissues to an interval exercise training regimen. As the reviewer mentioned, this hypothesis, in connection with the selected regimen, was incorrect. However, JoVE explicitly encourages researchers to also include data from experiments that are not necessarily "successful" to show the range of outcomes possible when performing the described protocol. For this reason, we chose to include this data. To emphasize this point, we added some text to the results section of the manuscript to clarify that this experiment did not yield the expected results.

<u>Reviewer 2</u>

1. The manuscript lists several limitations and a few alternative solutions for addressing these shortcomings. Many of these limitations arise from aspects of the commercially available platform that are not yet adapted to this new afterload method. Though two of the authors have interest in the company selling the EHT platform, it is nevertheless understandable that the manufacturing has not yet adapted to this new supplemental attribute.

On the other hand, the failure to provide a specific solution to the problem of the difference the base stiffness between the magnetically responsive posts and the control posts (0.91 vs. 0.6 mN/mm) is less justifiable. The authors should provide a specific non-magnetic insert description (material and dimensions) that successfully abrogates this difference in non-actuated post stiffness (i.e. achieves 0.91 mN/mm post stiffness with a nonmagnetic material). This material, and its source, should be included in the table of reagents/equipment.

We thank the reviewer for raising this very important point. We entirely agree that the difference in basal stiffness between the control posts and magnetically responsive posts should be eliminated. To achieve this, we have inserted (non-magnetic) polystyrene rod fragments into the control posts to increase their rigidity. The resulting stiffness for control posts reinforced with a 0.4 mm thick styrene cylinders was 0.84 mN/mm, which is very close to the basal stiffness of the magnetically responsive silicone posts (0.91 mN/mm). Please see Reviewer-Only Figure 1 for more detailed results. To instruct the reader on how to achieve this, a corresponding step has been added to the protocol. Also, the styrene rods used for this adaptation have been referenced in the material spreadsheet.

2. The representative results in Figures 7 and 8 should be more complete (similar to presentations in Reference 24) with inclusion of additional variables including work, rate of force generation, rate of force decay, etc.

   We thank the reviewer for this remark. We have included the suggested additional contractility data (force production rate, force decay rate, and work) in the new Supplementary Figures 2 and 3 and amended the manuscript to reflect these changes.
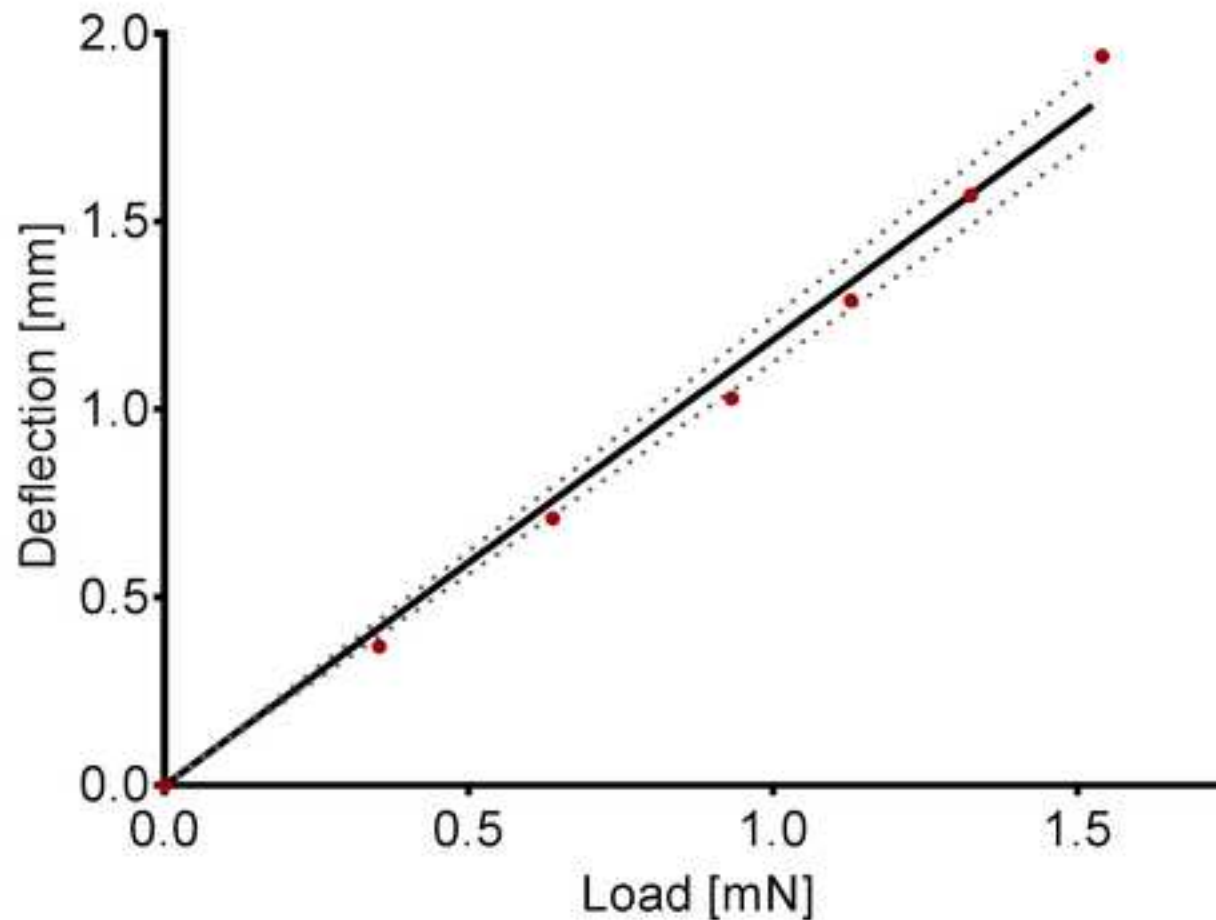
$$f(x) = 1.186x \rightarrow 1/m = 0.84$$

Reviewer-Only Figure 1: 5 styrene cylinders measuring 0.4 mm in diameter and 2 mm in height were stacked into a hollow silicone post. Stiffness k was determined optically for said silicone post by tracing the post deflection caused by 6 different test loads. The red dots represent the measured deflections, the solid black line displays the linear regression function plotted over the measured values with the dotted grey line indicating the 95% confidence interval for the regression function's slope. The stiffness measured for the given post setup was 0.84 mN/mm.
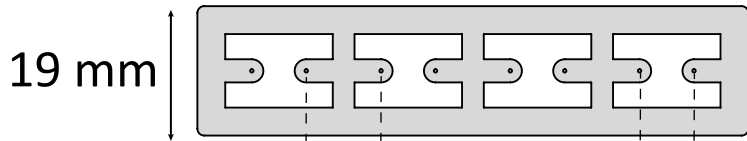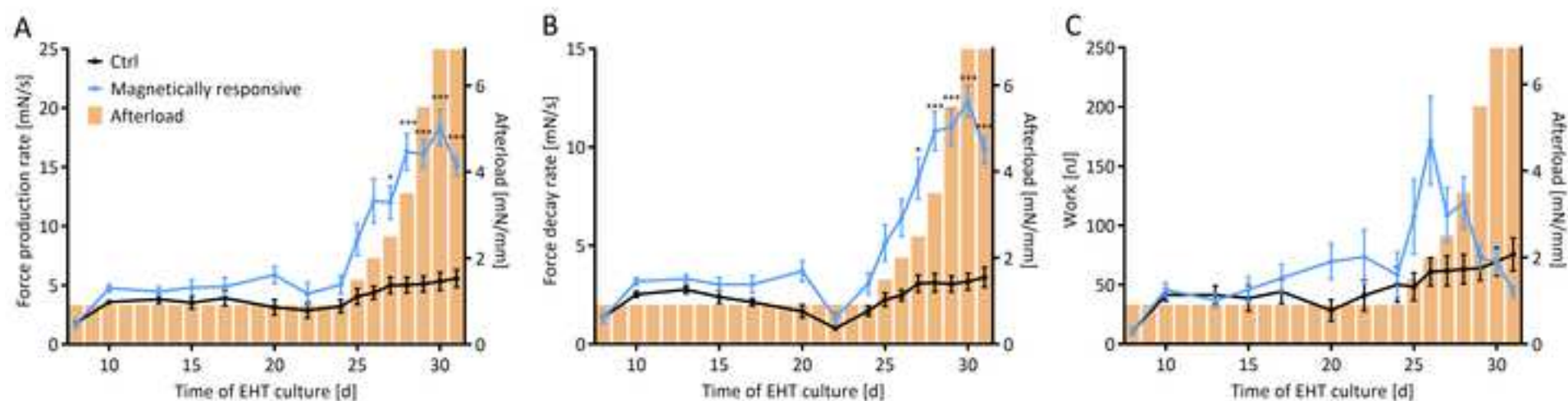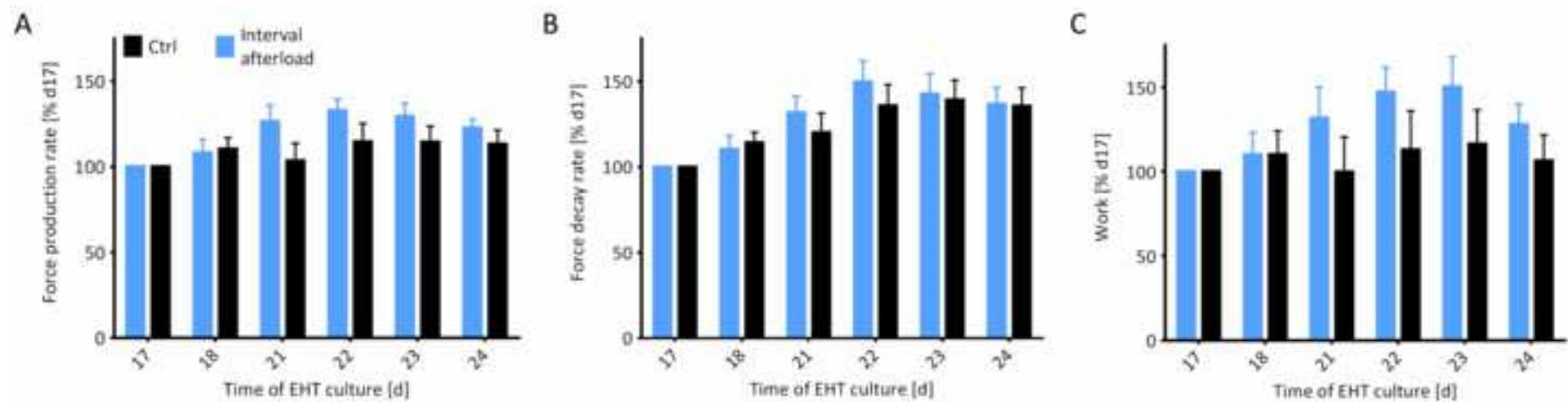
A

80 mm

19 mm

11.25 mm   8 mm

B

3 mm

12.5 mm

C

0.5 mm

1.3 mm

0.5mm

2.6 mm
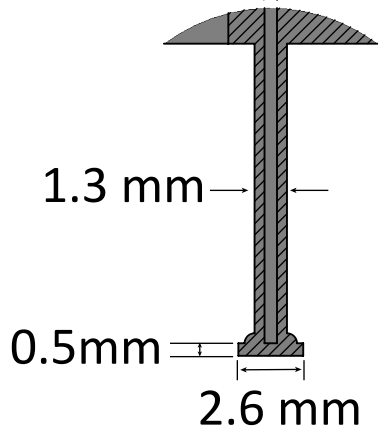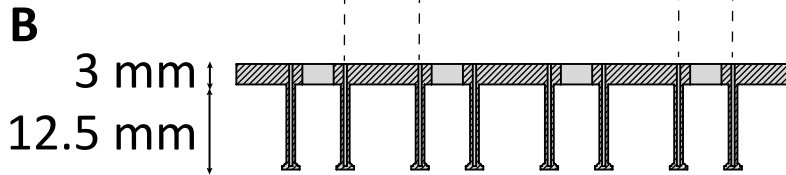
jove
1 Alewife Center #200
Cambridge, MA 02140
Tel: 617.945.9051
www.jove.com

ARTICLE AND VIDEO LICENSE AGREEMENT

Title of Article: | Magnetic adjustment of afterload in engineered heart tissues

Author(s): | Benjamin Becker*, Marita L. Rodriguez*, Tessa R. Werner, Justus Stenzig, Thomas Eschenhagen, Marc N. Hirt

Item 1: The Author elects to have the Materials be made available (as described at http://www.jove.com/publish) via:

☒ Standard Access   ☐ Open Access

Item 2: Please select one of the following items:

☒ The Author is **NOT** a United States government employee.

☐ The Author is a United States government employee and the Materials were prepared in the course of his or her duties as a United States government employee.

☐ The Author is a United States government employee but the Materials were NOT prepared in the course of his or her duties as a United States government employee.

ARTICLE AND VIDEO LICENSE AGREEMENT

1.   **Defined Terms.** As used in this Article and Video License Agreement, the following terms shall have the following meanings: "**Agreement**" means this Article and Video License Agreement; "**Article**" means the article specified on the last page of this Agreement, including any associated materials such as texts, figures, tables, artwork, abstracts, or summaries contained therein; "**Author**" means the author who is a signatory to this Agreement; "**Collective Work**" means a work, such as a periodical issue, anthology or encyclopedia, in which the Materials in their entirety in unmodified form, along with a number of other contributions, constituting separate and independent works in themselves, are assembled into a collective whole; "**CRC License**" means the Creative Commons Attribution-Non Commercial-No Derivs 3.0 Unported Agreement, the terms and conditions of which can be found at: http://creativecommons.org/licenses/by-nc-nd/3.0/legalcode; "**Derivative Work**" means a work based upon the Materials or upon the Materials and other pre-existing works, such as a translation, musical arrangement, dramatization, fictionalization, motion picture version, sound recording, art reproduction, abridgment, condensation, or any other form in which the Materials may be recast, transformed, or adapted; "**Institution**" means the institution, listed on the last page of this Agreement, by which the Author was employed at the time of the creation of the Materials; "**JoVE**" means MyJove Corporation, a Massachusetts corporation and the publisher of The Journal of Visualized Experiments; "**Materials**" means the Article and / or the Video; "**Parties**" means the Author and JoVE; "**Video**" means any video(s) made by the Author, alone or in conjunction with any other parties, or by JoVE or its affiliates or agents, individually or in collaboration with the Author or any other parties, incorporating all or any portion

of the Article, and in which the Author may or may not appear.

2.   **Background.** The Author, who is the author of the Article, in order to ensure the dissemination and protection of the Article, desires to have the JoVE publish the Article and create and transmit videos based on the Article. In furtherance of such goals, the Parties desire to memorialize in this Agreement the respective rights of each Party in and to the Article and the Video.

3.   **Grant of Rights in Article.** In consideration of JoVE agreeing to publish the Article, the Author hereby grants to JoVE, subject to **Sections 4** and **7** below, the exclusive, royalty-free, perpetual (for the full term of copyright in the Article, including any extensions thereto) license (a) to publish, reproduce, distribute, display and store the Article in all forms, formats and media whether now known or hereafter developed (including without limitation in print, digital and electronic form) throughout the world, (b) to translate the Article into other languages, create adaptations, summaries or extracts of the Article or other Derivative Works (including, without limitation, the Video) or Collective Works based on all or any portion of the Article and exercise all of the rights set forth in (a) above in such translations, adaptations, summaries, extracts, Derivative Works or Collective Works and(c) to license others to do any or all of the above. The foregoing rights may be exercised in all media and formats, whether now known or hereafter devised, and include the right to make such modifications as are technically necessary to exercise the rights in other media and formats. If the "Open Access" box has been checked in **Item 1** above, JoVE and the Author hereby grant to the public all such rights in the Article as provided in, but subject to all limitations and requirements set forth in, the CRC License.

612542.6   For questions, please contact us at submissions@jove.com or +1.617.945.9051.

4. **Retention of Rights in Article.** Notwithstanding the exclusive license granted to JoVE in **Section 3** above, the Author shall, with respect to the Article, retain the non-exclusive right to use all or part of the Article for the non-commercial purpose of giving lectures, presentations or teaching classes, and to post a copy of the Article on the Institution's website or the Author's personal website, in each case provided that a link to the Article on the JoVE website is provided and notice of JoVE's copyright in the Article is included. All non-copyright intellectual property rights in and to the Article, such as patent rights, shall remain with the Author.

5. **Grant of Rights in Video – Standard Access.** This **Section 5** applies if the "Standard Access" box has been checked in **Item 1** above or if no box has been checked in **Item 1** above. In consideration of JoVE agreeing to produce, display or otherwise assist with the Video, the Author hereby acknowledges and agrees that, Subject to **Section 7** below, JoVE is and shall be the sole and exclusive owner of all rights of any nature, including, without limitation, all copyrights, in and to the Video. To the extent that, by law, the Author is deemed, now or at any time in the future, to have any rights of any nature in or to the Video, the Author hereby disclaims all such rights and transfers all such rights to JoVE.

6. **Grant of Rights in Video – Open Access.** This **Section 6** applies only if the "Open Access" box has been checked in **Item 1** above. In consideration of JoVE agreeing to produce, display or otherwise assist with the Video, the Author hereby grants to JoVE, subject to **Section 7** below, the exclusive, royalty-free, perpetual (for the full term of copyright in the Article, including any extensions thereto) license (a) to publish, reproduce, distribute, display and store the Video in all forms, formats and media whether now known or hereafter developed (including without limitation in print, digital and electronic form) throughout the world, (b) to translate the Video into other languages, create adaptations, summaries or extracts of the Video or other Derivative Works or Collective Works based on all or any portion of the Video and exercise all of the rights set forth in (a) above in such translations, adaptations, summaries, extracts, Derivative Works or Collective Works and (c) to license others to do any or all of the above. The foregoing rights may be exercised in all media and formats, whether now known or hereafter devised, and include the right to make such modifications as are technically necessary to exercise the rights in other media and formats. For any Video to which this **Section 6** is applicable, JoVE and the Author hereby grant to the public all such rights in the Video as provided in, but subject to all limitations and requirements set forth in, the CRC License.

7. **Government Employees.** If the Author is a United States government employee and the Article was prepared in the course of his or her duties as a United States government employee, as indicated in **Item 2** above, and any of the licenses or grants granted by the Author hereunder exceed the scope of the 17 U.S.C. 403, then the rights granted hereunder shall be limited to the maximum rights permitted under such statute. In such case, all provisions contained herein that are not in conflict with such statute shall remain in full force and effect, and all provisions contained herein that do so conflict shall be deemed to be amended so as to provide to JoVE the maximum rights permissible within such statute.

8. **Protection of the Work.** The Author(s) authorize JoVE to take steps in the Author(s) name and on their behalf if JoVE believes some third party could be infringing or might infringe the copyright of either the Author's Article and/or Video.

9. **Likeness, Privacy, Personality.** The Author hereby grants JoVE the right to use the Author's name, voice, likeness, picture, photograph, image, biography and performance in any way, commercial or otherwise, in connection with the Materials and the sale, promotion and distribution thereof. The Author hereby waives any and all rights he or she may have, relating to his or her appearance in the Video or otherwise relating to the Materials, under all applicable privacy, likeness, personality or similar laws.

10. **Author Warranties.** The Author represents and warrants that the Article is original, that it has not been published, that the copyright interest is owned by the Author (or, if more than one author is listed at the beginning of this Agreement, by such authors collectively) and has not been assigned, licensed, or otherwise transferred to any other party. The Author represents and warrants that the author(s) listed at the top of this Agreement are the only authors of the Materials. If more than one author is listed at the top of this Agreement and if any such author has not entered into a separate Article and Video License Agreement with JoVE relating to the Materials, the Author represents and warrants that the Author has been authorized by each of the other such authors to execute this Agreement on his or her behalf and to bind him or her with respect to the terms of this Agreement as if each of them had been a party hereto as an Author. The Author warrants that the use, reproduction, distribution, public or private performance or display, and/or modification of all or any portion of the Materials does not and will not violate, infringe and/or misappropriate the patent, trademark, intellectual property or other rights of any third party. The Author represents and warrants that it has and will continue to comply with all government, institutional and other regulations, including, without limitation all institutional, laboratory, hospital, ethical, human and animal treatment, privacy, and all other rules, regulations, laws, procedures or guidelines, applicable to the Materials, and that all research involving human and animal subjects has been approved by the Author's relevant institutional review board.

11. **JoVE Discretion.** If the Author requests the assistance of JoVE in producing the Video in the Author's facility, the Author shall ensure that the presence of JoVE employees, agents or independent contractors is in accordance with the relevant regulations of the Author's institution. If more than one author is listed at the beginning of this Agreement, JoVE may, in its sole

ARTICLE AND VIDEO LICENSE AGREEMENT

discretion, elect not take any action with respect to the Article until such time as it has received complete, executed Article and Video License Agreements from each such author. JoVE reserves the right, in its absolute and sole discretion and without giving any reason therefore, to accept or decline any work submitted to JoVE. JoVE and its employees, agents and independent contractors shall have full, unfettered access to the facilities of the Author or of the Author's institution as necessary to make the Video, whether actually published or not. JoVE has sole discretion as to the method of making and publishing the Materials, including, without limitation, to all decisions regarding editing, lighting, filming, timing of publication, if any, length, quality, content and the like.

12.   **Indemnification.** The Author agrees to indemnify JoVE and/or its successors and assigns from and against any and all claims, costs, and expenses, including attorney's fees, arising out of any breach of any warranty or other representations contained herein. The Author further agrees to indemnify and hold harmless JoVE from and against any and all claims, costs, and expenses, including attorney's fees, resulting from the breach by the Author of any representation or warranty contained herein or from allegations or instances of violation of intellectual property rights, damage to the Author's or the Author's institution's facilities, fraud, libel, defamation, research, equipment, experiments, property damage, personal injury, violations of institutional, laboratory, hospital, ethical, human and animal treatment, privacy or other rules, regulations, laws, procedures or guidelines, liabilities and other losses or damages related in any way to the submission of work to JoVE, making of videos by JoVE, or publication in JoVE or elsewhere by JoVE. The Author shall be responsible for, and shall hold JoVE harmless from, damages caused by lack of sterilization, lack of cleanliness or by contamination due to

the making of a video by JoVE its employees, agents or independent contractors. All sterilization, cleanliness or decontamination procedures shall be solely the responsibility of the Author and shall be undertaken at the Author's expense. All indemnifications provided herein shall include JoVE's attorney's fees and costs related to said losses or damages. Such indemnification and holding harmless shall include such losses or damages incurred by, or in connection with, acts or omissions of JoVE, its employees, agents or independent contractors.

13.   **Fees.** To cover the cost incurred for publication, JoVE must receive payment before production and publication of the Materials. Payment is due in 21 days of invoice. Should the Materials not be published due to an editorial or production decision, these funds will be returned to the Author. Withdrawal by the Author of any submitted Materials after final peer review approval will result in a US$1,200 fee to cover pre-production expenses incurred by JoVE. If payment is not received by the completion of filming, production and publication of the Materials will be suspended until payment is received.

14.   **Transfer, Governing Law.** This Agreement may be assigned by JoVE and shall inure to the benefits of any of JoVE's successors and assignees. This Agreement shall be governed and construed by the internal laws of the Commonwealth of Massachusetts without giving effect to any conflict of law provision thereunder. This Agreement may be executed in counterparts, each of which shall be deemed an original, but all of which together shall be deemed to me one and the same agreement. A signed copy of this Agreement delivered by facsimile, e-mail or other means of electronic transmission shall be deemed to have the same legal effect as delivery of an original signed copy of this Agreement.

A signed copy of this document must be sent with all new submissions. Only one Agreement is required per submission.

CORRESPONDING AUTHOR

Name: Marc N. Hirt

Department: Insitute of Experimental Pharmacology and Toxicology

Institution: University Medical Center Hamburg-Eppendorf

Title: MD, PhD

Signature: _____   Date: 2019, Sept 23rd

Please submit a **signed** and **dated** copy of this license by one of the following three methods:
1.   Upload an electronic version on the JoVE submission site
2.   Fax the document to +1.866.381.2236
3.   Mail the document to JoVE / Attn: JoVE Editorial / 1 Alewife Center #200 / Cambridge, MA 02140

612542.6   For questions, please contact us at submissions@jove.com or +1.617.945.9051.